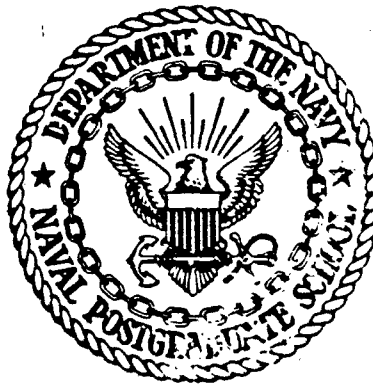


AD-A156 145

NAVAL POSTGRADUATE SCHOOL

Monterey, California



Reproduced From
Best Available Copy

DTIC
ELECTE
JUL 03 1985
S D G

THESIS

EFFECT OF PRIOR WARM ROLLING ON THE RETAINED
AUSTENITE CONTENT AND HARDENING RESPONSE OF
(VIM-VAR) AISI M-50 STEEL

by

Nestor H. Camerino, Jr.

March 1985

Thesis Advisor:

T. R. McNelley

DTIC FILE COPY

Approved for public release; distribution is unlimited

20000811022

85

6 10 045

SECURITY CLASSIFICATION OF THIS PAGE (When Data Entered)

REPORT DOCUMENTATION PAGE		READ INSTRUCTIONS BEFORE COMPLETING FORM
1. REPORT NUMBER	2. GOVT ACCESSION NO. AD-A156145	3. RECIPIENT'S CATALOG NUMBER
4. TITLE (and Subtitle) Effect of Prior Warm Rolling on the Retained Austenite Content and Hardening Response of (VIM-VAR) AISI M-50 Steel		5. TYPE OF REPORT & PERIOD COVERED Master's Thesis; March 1985
		6. PERFORMING ORG. REPORT NUMBER
7. AUTHOR(s) Nestor H. Camerino, Jr.		8. CONTRACT OR GRANT NUMBER(s)
9. PERFORMING ORGANIZATION NAME AND ADDRESS Naval Postgraduate School Monterey, CA 93943		10. PROGRAM ELEMENT, PROJECT, TASK AREA & WORK UNIT NUMBERS
11. CONTROLLING OFFICE NAME AND ADDRESS Naval Postgraduate School Monterey, CA 93943		12. REPORT DATE March 1985
		13. NUMBER OF PAGES 46 pages
14. MONITORING AGENCY NAME & ADDRESS (if different from Controlling Office)		15. SECURITY CLASS. (of this report) Unclassified
		15a. DECLASSIFICATION/DOWNGRADING SCHEDULE
16. DISTRIBUTION STATEMENT (of this Report) Approved for public release; distribution is unlimited		
17. DISTRIBUTION STATEMENT (of the abstract entered in Block 20, if different from Report)		
18. SUPPLEMENTARY NOTES		
19. KEY WORDS (Continue on reverse side if necessary and identify by block number) Retained Austenite		
20. ABSTRACT (Continue on reverse side if necessary and identify by block number) The objective of warm rolling M-50 bearing steel is microstructural refinement which may lead to increases in rolling contact fatigue life. A consequence of this refinement is that the austenitizing temperature used in the final hardening cycle should be reduced. This is because warm rolling leads to faster dissolution of finer soluble carbides at the austenitizing temperature. This thesis effort		

DD FORM 1473
1 JAN 73

EDITION OF 1 NOV 65 IS OBSOLETE
S/N 0102-LF-014-6401

SECURITY CLASSIFICATION OF THIS PAGE (When Data Entered)

20. (Continued)

determined the temperature decrease that warm rolling allows in austenitizing to produce a microstructure of finer grain and carbide size but equivalent carbide dissolution. Here, this has been inferred by measurement of the volume fraction of retained austenite in the as-hardened microstructure, retained austenite being a function of the amount of carbides taken into solution during austenitization. It was found that the standard austenitizing temperature of 1106°C used to harden stock M-50 can be reduced by 63 centigrade degrees with warm-rolled M-50 steel.

Accession For	
NTIS GRA&I	<input checked="" type="checkbox"/>
DTIC TAB	<input type="checkbox"/>
Unannounced	<input type="checkbox"/>
Justification	
By _____	
Distribution/	
Availability Codes	
Dist	Avail and/or Special
A/1	

Approved for public release; distribution is unlimited

Effect of Prior Warm Rolling on the Retained
Austenite Content and Hardening Response
of (VIM-VAR) AISI M-50 Steel

by

Nestor H. Camerino, Jr.
Lieutenant, United States Navy
B.S.M.E., United States Naval Academy, 1979

Submitted in partial fulfillment of the
requirements for the degree of

MASTER OF SCIENCE IN MECHANICAL ENGINEERING

from the

NAVAL POSTGRADUATE SCHOOL
March 1985

Author:

Nestor H. Camerino, Jr.

Nestor H. Camerino, Jr.

Approved by:

T. B. McNelley

T. B. McNelley, Thesis Advisor

P. J. Marto

P. J. Marto, Chairman, Department
of Mechanical Engineering

J. N. Dyer

J. N. Dyer, Dean of Science and Engineering

ABSTRACT

The objective of warm rolling M-50 bearing steel is microstructural refinement which may lead to increases in rolling contact fatigue life. A consequence of this refinement is that the austenitizing temperature used in the final hardening cycle should be reduced. This is because warm rolling leads to faster dissolution of finer soluble carbides at the austenitizing temperature. This thesis effort determined the temperature decrease that warm rolling allows in austenitizing to produce a microstructure of finer grain and carbide size but equivalent carbide dissolution. Here, this has been inferred by measurement of the volume fraction of retained austenite in the as-hardened microstructure, retained austenite being a function of the amount of carbides taken into solution during austenitization. It was found that the standard austenitizing temperature of 1106°C used to harden stock M-50 can be reduced by 63 centigrade degrees with warm-rolled M-50 steel.

TABLE OF CONTENTS

I.	INTRODUCTION	9
II.	EXPERIMENTAL PROCEDURE	14
A.	HEAT TREATMENT	16
1.	Hardening	16
2.	Tempering	17
B.	SURFACE PREPARATION	18
1.	Mechanical Polishing	18
2.	Electropolishing	18
C.	X-RAY DIFFRACTOMETRY	22
1.	Equipment Description	22
2.	Calculating Retained Austenite	23
III.	RESULTS AND DISCUSSION	32
IV.	CONCLUSIONS AND RECOMMENDATIONS	42
A.	CONCLUSIONS	42
B.	RECOMMENDATIONS	42
	LIST OF REFERENCES	43
	INITIAL DISTRIBUTION LIST	45

LIST OF TABLES

I.	COMPOSITION OF M-50 STEEL	14
II.	R-FACTOR SAMPLE CALCULATIONS: MARTENSITE	29
III.	R-FACTOR SAMPLE CALCULATIONS: AUSTENITE	30
IV.	SAMPLE CALCULATION OF ERROR IN RA	41

LIST OF FIGURES

- 1.1 The trend in the Dynamic Number (DN), in bearing design has been upwards. D is the bore diameter and N the speed of rotation in RPM. Each point in this diagram represents a specific engine design. Figure courtesy of NAPC . . . 9

- 1.2 Operating at higher DN has shortened bearing life and switched the principle failure mode from fatigue to fracture. Figure courtesy of NAPC . . . 10

- 2.1 A schematic of the schedule of operations in thermomechanical processing which begins with an initial heat treatment to back the material out of the spheroidize-annealed condition and then warm rolling to develop refined carbide and ferrite grain sizes . . . 15

- 3.1 Retained Austenite (RA) as a function of austenitizing temperature for test samples quenched into molten salt at 620°C prior to air cooling to room temperature. Warm-rolled material retains more austenite in the as-quenched condition than as-received material for all austenitizing temperatures . . . 34

- 3.2 Retained Austenite (RA) as a function of austenitizing temperature for test samples directly quenched in water to room temperature. Warm-rolled material retains more austenite in the as-quenched condition than as-received material for all austenitizing temperatures . . . 35

- 3.3 Tempering responses of the warm-rolled sample austenitized at 1043°C and the as-received sample austenitized at 1108°C. To within experimental accuracy, they are identical especially where the secondary hardening peak occurs at 61.5 Rockwell C and 540°C . . . 38

- 3.4 Tempering responses of the warm-rolled and as-received samples austenitized at 1043°C. Though only slightly so, the as-received sample is consistently softer . . . 40

ACKNOWLEDGEMENT

I would like to thank Professor Terry R. McNelley for providing valuable advice and guidance during the course of this work. Additionally, I would like to express my appreciation for the outstanding technical support provided by Mr. Tom Kellogg in the way of equipments and materials operation and procurement.

I would like also to acknowledge the Naval Air Propulsion Center, Trenton, New Jersey, and Mr. Dan Popgoshev for providing the funding for this research. Last but not least, I would like to acknowledge the Air Force Wright Aeronautical Laboratories, Wright Patterson Air Force Base, Dayton, Ohio, and Mr. Ron Dayton for funding to continue research in this area.

I. INTRODUCTION

As illustrated in Figure 1.1, the trend in recent years has been to design gas turbine engine bearings on ever increasing Dynamic Numbers, DN. It is readily apparent that for a fixed bore diameter, D , this equates to higher speeds of rotation, N . Higher operating speeds, of course, results in the development of greater Hertzian stresses within the bearings, and as shown in Figure 1.2, shortened bearing life

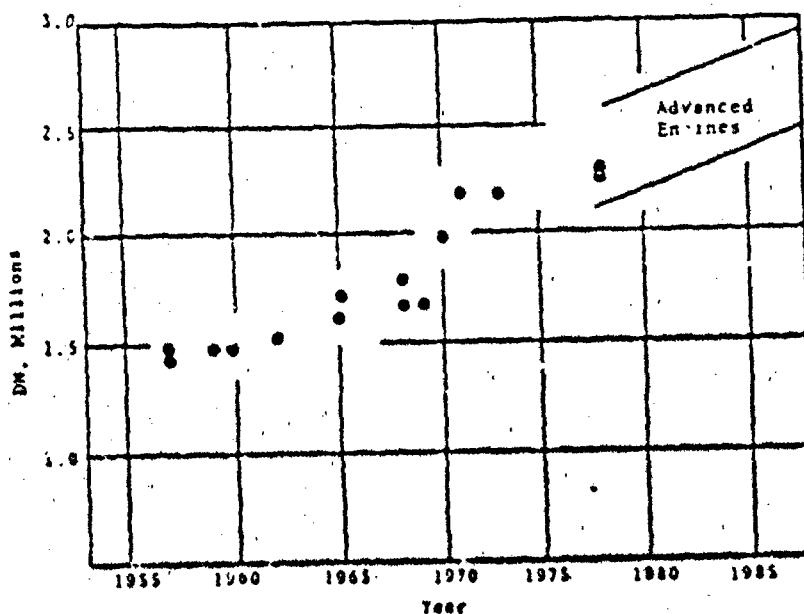


Figure 1.1. The trend in the Dynamic Number (DN), in bearing design has been upwards. D is the bore diameter and N the speed of rotation in RPM. Each point in this diagram represents a specific engine design. Figure courtesy of NAPC.

accompanied by a switch in the expected principle failure mode from fatigue to fracture.

Mainshaft Bearing Lives & Expected Failure Mode as a Function of Speed For a Constant Bore Size

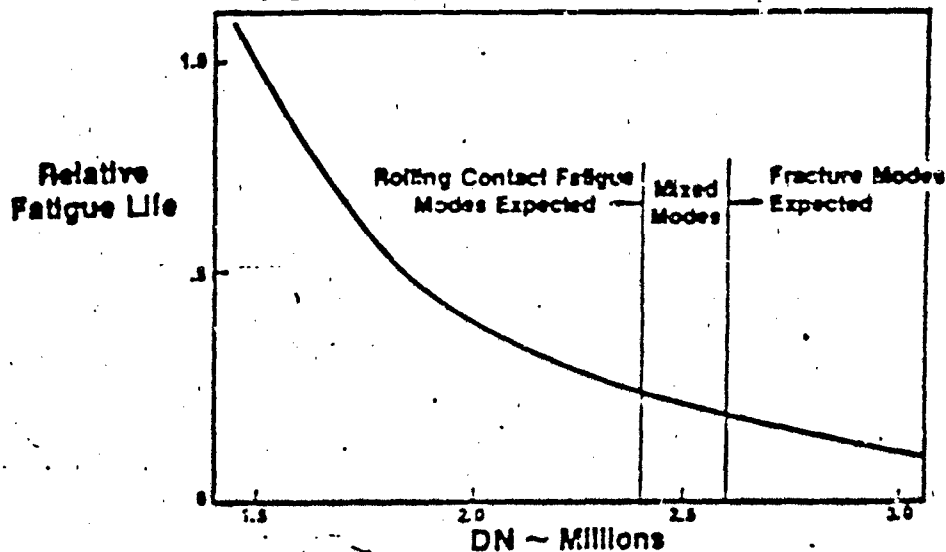


Figure 1.2. Operating at higher DN has shortened bearing life and switched the principle failure mode from fatigue to fracture. Figure courtesy of NAPS.

The problem of diminished bearing life with increasing operating speeds has led to an interest in methods to improve the mechanical properties of AISI M-50 steel from which gas turbine engine main shaft bearings are made. Some methods have included powder metallurgy, rapid solidification processing, and carburizing. Of these methods only carburizing has shown some success. The method

chosen for investigation at the Naval Postgraduate School is thermomechanical processing. Through warm rolling, microstructural refinement is developed in the material before the final hardening. It was expected that such a process would result in an improvement in the rolling contact fatigue life of gas turbine bearings made from this steel.

Sherby [Ref. 1] showed that ultra-high carbon steels can be superplastically deformed by warm rolling at temperatures between $0.4 T_m$ to $0.7 T_m$. This thermomechanical process, which is essentially an annealing heat treatment with concurrent plastic deformation, was shown by Sherby to enhance spheroidization and result in much refined carbide and ferrite grain sizes. McNelley, et. al. [Ref. 2] applying this technique to 52100 bearing steel, showed that the resultant microstructural refinement led to an increase in the yield strength and fracture toughness in 52100 steel. At the Naval Postgraduate School, Larson [Ref. 5] adapted the technique to AISI M-50 steel and showed that M-50 steel can be successfully warm rolled at 700°C to a true strain of -2.0 and that the resulting refined microstructure leads to an increase in its ultimate tensile strength. Bres [Ref. 7] continuing Larson's work at the Naval Postgraduate School, showed that the microstructural refinement persists through final hardening and that warm-rolled is harder than as-received M-50 for austenitizing temperatures up to 1108°C .

Following Bres' work, Butterfield [Ref. 6] processed and then fatigue tested rolling contact test rods machined from both warm-rolled and as-received M-50. Based on initial investigations by Bres, a hardening temperature of 1036°C and a hardening time of first five and then two minutes was thought to be appropriate for use with warm-rolled M-50. Until this research, no specific investigation had been made to determine an appropriate austenitizing temperature. This is where the work for this thesis began; the objective of this work was to find an austenitizing temperature to use in the final hardening cycle of warm-rolled M-50 steel. It was assumed in this work that austenitizing of the previously warm-rolled material should be done at a temperature such that the same carbon content would be attained as in the as-received material. This temperature would be lower than that used with as-received material and would thus allow retention of the refinement due to previous rolling. The principle experimental method to accomplish this task was X-Ray diffractometry. The experimental method is based on the assumption that if two samples contain the same volume fractions of retained austenite in the as-quenched condition, then those two samples took into solution equivalent amounts of principally carbon and secondarily other alloying elements during hardening. The experimental procedure, then, was to austenitize test samples of warm-rolled and

as-received M-50 together over a range of austenitizing temperatures and then to measure and compare the volume fractions of retained austenite between the samples. Finally, hardness and tempering tests would be made to compare properties between samples after hardening.

II. EXPERIMENTAL PROCEDURE

The material for this work was obtained from a commercial bearing manufacturer as a bar from a vacuum-induction melted, vacuum-arc remelted (VIM-VAR) heat of M-50, hot rolled to bar of 44.5 mm diameter. The as-received bar of M-50 was in a spheroidize-annealed condition and of composition given in Table I.

TABLE I
COMPOSITION OF M-50 STEEL

C	Mn	Si	Cr	Mo	V
0.80	0.30	0.25	4.10	4.25	1.10

Test samples were rectangular coupons transversely sectioned from the full diameter of the as-received bar and from lengths of the thermomechanically processed material. Nominal dimensions of all coupons was 19 mm by 16 mm by 3.2 mm, with the long dimension longitudinal to the direction of rolling. A 1.6 mm diameter hole was drilled

near one end so that coupons could be wired together and handled during heat treatment.

Thermomechanical processing is essentially a two-step operation, initial heat treatment and subsequent warm rolling. Following the scheduled procedures developed by Larson [Ref. 3] and given by Figure 2.1, as-received bar was

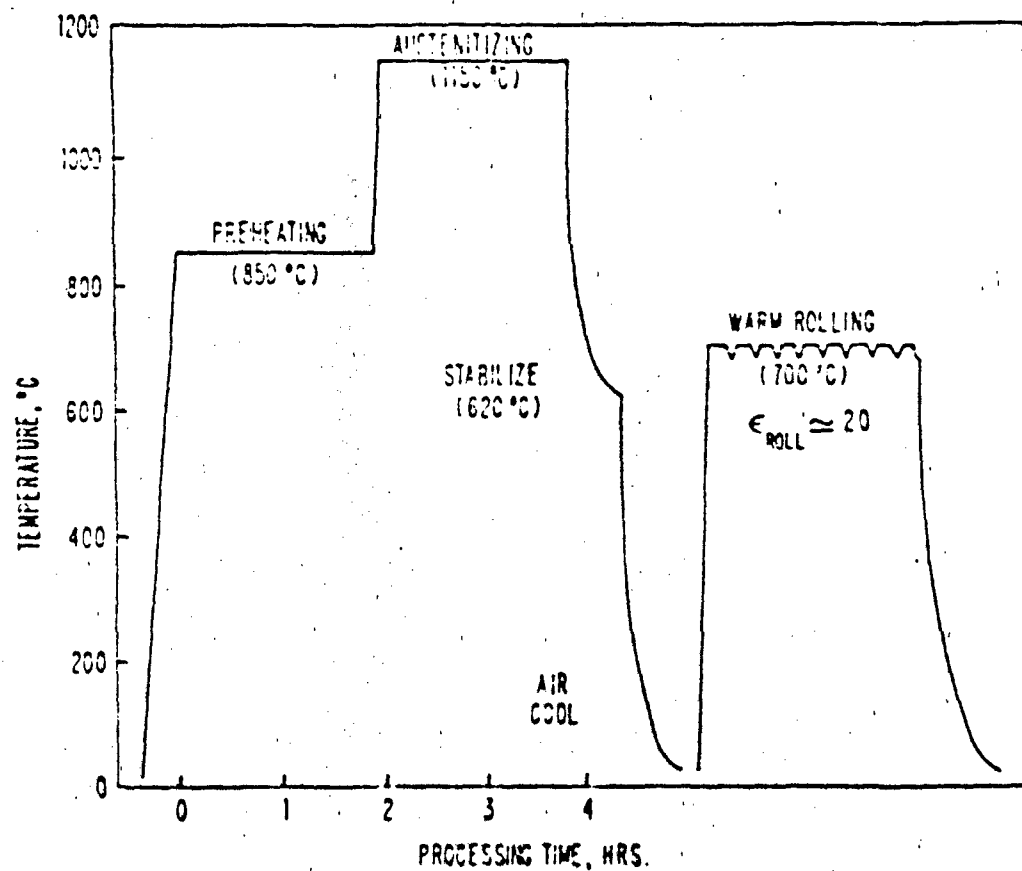


Figure 2.1. A schematic of the schedule of operations in thermomechanical processing which begins with an initial heat treatment to back the material out of the spheroidize-annealed condition and then warm rolling to develop refined carbide and ferrite grain sizes.

heat treated to back it out of the spheroidize-annealed condition and then isothermally rolled at 700°C, on unheated rolls and with reheating between passes, to a true strain of about -2.0 (86 pct reduction in area). As-received M-50 thermomechanically processed in this manner had a hardness of 39 Rockwell C as compared to 19 Rockwell C for unprocessed M-50.

A. HEAT TREATMENT

As-received and warm-rolled coupons were wired together in pairs with Nichrome wire so that each would receive identical heat treatment.

1. Hardening

Coupon pairs were austenitized at 993, 1006, 1043, 1053 and 1108°C, with temperature control to $\pm 10^\circ\text{C}$. Each pair was preheated for seven minutes at 850°C in an electrically-fired box furnace. The pair was then transferred to a molten salt bath and held for 2 minutes 15 seconds for austenitization at one of the five above-mentioned temperatures. This was followed by a 45 second molten salt quench at 620°C to inhibit carbide precipitation along austenite grain boundaries. Finally, the pair was allowed to air cool to room temperature which was 20°C in all cases. An identical procedure was carried out with as-received/warm-rolled pairs that were austenitized concurrently with the samples just described except that

this second set of samples was quenched directly into water at room temperature, 20°C. Where it is not otherwise mentioned, austenitizing times were as stated here.

2. Tempering

The as-received coupon austenitized at 1108°C and the warm-rolled and the as-received coupons austenitized at 1043°C were tempered. These three coupons had been through the molten salt quench at 620°C prior to air cooling to room temperature. The secondary hardening response of the as-received material austenitized at 1108°C, and the warm-rolled material austenitized at 1043°C, were compared directly since both coupons contained about the same volume fraction of retained austenite in the as-quenched condition. The secondary hardening response of the as-received material austenitized at 1043°C was compared with that of the warm-rolled material austenitized at 1043°C.

The coupons were sectioned into six pieces nominally 6.4 mm by 6.4 mm. They were then frozen in liquid Nitrogen for one hour to decompose any retained austenite. The pieces of as-received coupons austenitized at 1108°C and the pieces of warm-rolled material austenitized at 1043°C were wrapped together in pairs in Nickel foil with Titanium sponge added and foils sealed to help minimize decarburization during tempering. Tempering was done at each of six different temperatures for two hours at temperature in

electrically-fired box furnaces. Temperatures were 180, 350, 450, 540, 620, and 680°C, with temperature control to $\pm 5^\circ\text{C}$. After tempering, the pieces were wet-ground successively on 240, 320, 400, and 600 grit papers to remove scale and the possibly decarburized surface layer.

Hardness was then measured on a Wilson Rockwell Hardness testing machine. The resultant tempering response was then displayed as hardness versus tempering temperature.

B. SURFACE PREPARATION

After austenitization and before X-Ray diffraction, one face of each coupon was mechanically and then electrolytically polished.

1. Mechanical Polishing

Polishing began with wet grinding on a Buehler motor-driven belt grinder using 180 grit paper to remove scale and the possibly decarburized surface layer. About 0.03 cm was removed by this coarse grinding. Successive wet grinding by hand on 240, 320, 400, and 600 grit paper then followed. Coupons were subsequently polished on motor-driven polishing wheels using a 1.0 micron and then a 0.5 micron Alpha Alumina micropolish followed by a 0.05 micron Gamma Alumina micropolish to produce a mirror finish.

2. Electropolishing

Thermal and/or mechanical stresses developed during mechanical polishing can cause retained austenite to

transform into martensite in the near-surface layers and so lead to inaccurate retained austenite measurements. Electropolishing was done to remove the disturbed surface layer that is inevitable in even the most careful mechanical polishing.

The backside and edges of the coupons were masked with teflon tape to allow electropolishing of just the mechanically polished face. It was observed that electropolishing occurs preferentially at edges. These areas are not scanned during X-Ray diffraction and do not need to be electropolished. Consequently, masking the edges allowed for a more concentrated electropolishing of the appropriate surface. In general, masking allowed the use of lower voltages and amperages to produce adequate current densities to do the job. Otherwise, overheating of the coupons and of the electrolyte resulted. There was concern that such overheating might decompose some retained austenite. Additionally, since the electrolyte contained perchloric acid, it was advisable to keep its temperature below 29°C. A 1.6 mm Type K Chromel-Alumel thermocouple connected to a Newport digital pyrometer was attached to a coupon via the 1.6 mm hole to check for the maximum temperature reached during electropolishing. This maximum temperature of 75°C along with the short electropolishing time was not considered sufficient to temper the retained austenite.

An electrolyte of the following composition was used: 70 ml Perchloric acid (60%), 140 ml distilled water, 700 ml Ethanol (195 proof), and 70 ml Butyl Cellusolve. A volume of 750 ml of electrolyte was placed in an 800 ml Pyrex beaker, with moderate agitation provided by a magnetic stirrer.

The starting temperature of the electrolyte was nominally 20°C. It was observed that an electrolyte bath temperature of 14°C would cause a transformation of retained austenite to martensite. This was observed as a significant decrease in the integrated intensities of austenite peaks and a corresponding rise in the integrated intensities of martensite peaks on X-Ray diffraction patterns as compared to the same sample that had previously been electropolished in an electrolyte at a starting temperature of 20°C.

A current density of 3.0 amps per square cm was enough to remove 0.003 cm from the surface in 80 seconds. Thinning of the coupons by electropolishing could not be measured with a micrometer so an indirect method was used to estimate the amount of surface removed. A Metler balance was used to find the mass of the coupons before and after electropolishing. Then with the density of M-50, an estimate was made of the thickness of surface metal removed by electropolishing.

A stainless steel strip was used as the cathode. It was separated from the anode or coupon by about 2.5 cm.

Direct current was provided by a Buehler Electromet polisher machine.

X-Ray diffraction patterns were run on several test coupons before and after electropolishing so that quantitative comparisons could be made of its effect on the calculated volume fraction of retained austenite. For example, this was done with a warm-rolled test coupon that had been austenitized at 1108°C and quenched in molten salt prior to air cooling to room temperature. Before electropolishing the measured volume fraction of retained austenite was 15.8% as compared to 25.4% after electropolishing. This is a difference of 9.6% and would suggest that mechanical polishing induces stresses that causes decomposition of the retained austenite in the near-surface layers.

Another benefit apparently attributable to electropolishing is that it reduced the degree of preferred orientation on the polished faces of the coupons. For example, two warm-rolled coupons showed 65% and 33% decreases after electropolishing. This result would suggest that mechanical polishing may have induced a higher level of preferred orientation than had originally been caused by rolling in the manufacture and latter by the extensive warm rolling in thermomechanical processing.

The adequacy of the electropolishing was checked by comparing the X-Ray diffraction patterns produced by coupons

that were only mechanically polished with the same coupons after one and two electropolishing treatments. The second electropolishing produced no change in the X-Ray diffraction patterns so that the removal of about 0.003 cm of metal was considered sufficient to remove the disturbed surface layer.

C. X-RAY DIFFRACTOMETRY

1. Equipment Description

X-Ray diffraction patterns were obtained on the test coupons using a Philips X-Ray diffractometer consisting of a Model 3100 X-Ray Generator, Model 42267/0 Goniometer and Philips Data Control and Processor. All patterns were run using a Model 1601-4300 Graphite Crystal Diffracted Beam Monochromator in conjunction with a Cu-target X-Ray tube. The monochromator served to filter out all wavelengths except for the Cu K_{α} and was especially effective in filtering the fluorescent radiation from the iron of the coupons. The radiation wavelength was taken as 1.54178×10^{-8} cm, that is the weighted average of the K_{α_1} and K_{α_2} doublet.

Power settings at 40 KV and 30 mA provided a total power of 1200 VA that was well below the 1800 VA rating of the tube. These settings also produced a very good signal-to-noise ration. The data processor was set with a time constant of one second.

2. Calculating Retained Austenite

Quantitative determination of volume fractions of retained austenite in the as-quenched test coupons was by the direct comparison method. Briefly, the method is based on the principle that the X-Ray intensity diffracted from each phase present in a crystalline substance is proportional to the volume fraction of that phase. For materials with no preferred orientation, comparison of the diffracted intensities produced by single (hkl) planes of one phase with that produced by a second phase will accurately establish the volume fraction of each phase. Because of preferred orientation in the test coupons in this work, three austenite peaks and two martensite peaks were used for comparison. Through averaging, the error introduced by preferred orientation is minimized by the use of multiple peaks in the manner described in the SAE Manual SP-453 which details the procedural techniques in retained austenite measurement through X-Ray diffractometry [Ref. 4]. Throughout this work extensive use was made of this manual for guidance on the standardized methods in these type measurements. B. D. Cullity's text, Elements of X-Ray Diffraction, was the source of Tables, Appendices, and Figures of data required in the calculation of theoretical relative intensity factors, R.

a. Integrated Intensity from Diffraction Peaks

A range of 2θ from 49 to 93 degrees was scanned to obtain Bragg reflections from the desired crystallographic planes. These were the {200}, {220}, and {311} austenite and the {002-200}, and {112-211} martensite planes. The peaks produced by these planes were well defined and separated and except for the {002-200} martensite doublet, free from overlap and apparent carbide interference. This, of course, made them especially convenient for area measurements by planimeter. In the as-quenched condition, carbide interference with the {002-200} martensite doublet caused an asymmetry in the shape of the peak that was at first thought to be caused by overlap of the {002} and {200} reflections. As such, tempering would have eliminated the asymmetry as the body-centered tetragonal martensite relaxed into a much less strained body-centered cubic arrangement. Subsequent tempering, in fact, produced the expected {200} body centered cubic martensite peak and, unexpectedly, an unidentified but distinct carbide peak immediately alongside the martensite peak. Apparently the asymmetry in the {002-200} martensite doublet was caused by carbide interference and not by the overlap of the {002-200} peaks of the doublet.

As was expected, tempering resulted in a measurable narrowing of the relatively broad-based

diffraction peaks of body-centered tetragonal martensite. This was useful in ascertaining whether other carbide peaks might have been buried under that portion of the body-centered tetragonal martensite peaks uncovered by tempering. No other such carbides were evident. Tempering for this purpose was done for two hours at 540°C with an as-received coupon that had been austenitized at 993°C for two minutes and then quenched in molten salt at 620°C prior to air cooling to room temperature at 20°C. The coupon contained only 6.72 volume percent retained austenite and no measurable amount afterwards. The apparent freedom of the {200}, {220}, and {311} austenite peaks from carbide interference was evident from the lack of carbide activity at the 2θ positions previously occupied by the austenite peaks.

The integrated intensities of the three austenite and two martensite peaks were determined by measuring the areas above background with a planimeter. Background levels were typically 5 counts as opposed to 40 counts and greater for the austenite and martensite peaks.

Electropolishing was able to partially resolve the carbide interference with the {002-200} martensite doublet so that accurate measurement of that amount of area directly attributable to just the doublet could be made.

The {002-200} and {112-211} martensite doublet could not be resolved into their component peaks on the X-Ray diffraction patterns.

Scanning was done at a rate of one degree in 20 per minute and full scale was set at 500 counts per second.

b. Equations

The following equation was used to calculate the volume fraction of retained austenite:

$$R.A. = \left\{ \left(\frac{1}{n_A} \sum (I_{hkl_A} / R_{hkl_A}) \right) / \left(\frac{1}{n_A} \sum (I_{hkl_A} / R_{hkl_A}) + \frac{1}{n_M} \sum (I_{hkl_M} / R_{hkl_M}) \right) \right\} \quad (\text{eqn. 2.1})$$

where:

I_{hkl_A} , I_{hkl_M} integrated intensity of each austenite or martensite diffraction peak; equal to the area under the peak above background

R_{hkl_A} , R_{hkl_M} theoretical relative intensity factors used to scale I_{hkl_A} and I_{hkl_M}

n_A , n_M number of austenite and martensite peaks

Equation (2.1) is based on the assumption that only two phases are present in the as-quenched material, namely, austenite and martensite, according to the relation:

$$V_A + V_M = 1 \quad (\text{eqn. 2.2})$$

where

V_A, V_M are volume fractions of austenite and martensite.

The carbide fraction was neglected because carbide peaks could not be identified on the X-Ray diffraction patterns. A discussion of the probable magnitude of the resultant error in the retained austenite figures is included in later text. It is believed that the figures are just nominally higher than is actually the case. For the purposes of this investigation, since relative volume fractions of retained austenite in as-received as compared to warm-rolled material was what was sought, the assumption of a two phase composition was considered appropriate.

Theoretical intensity factors of R-factors, for each diffraction peak used was calculated from:

$$R = 1/v^2 (FF * p * LP) e^{-2M} \quad (\text{eqn. 2.3})$$

where:

$1/v^2$ reciprocal of the square of the volume of a unit cell

$FF = \{E(f - \Delta f)\}^2$ structure factor
 f atomic scattering factor
 Δf correction for anomalous scattering
 E # atoms per unit cell, 4 for FCC
 2 for BCC

P multiplicity factor of the (hkl) reflection

$LP = \{(1 + \cos^2 2A \cos^2 2\theta) / (\sin^2 \theta \cos \theta (1 + \cos^2 2A))\}$
 $A = 13.305$ angle of graphite monochromator crystal
 LP = Lorentz Polarization factor

e^{-2M} Debye-Waller or temperature factor

Sample calculations of the R-factors for the {002-200} martensite doublet and {200} austenite peak are given in Tables II and III.

Since the martensite doublets {002-200} and {112-211} could not be resolved into their component peaks, structure factors and multiplicities were calculated on the basis of a body-centered cubic martensite. This is standard practice in these cases and in effect, adds together the integrated intensities of the two peaks of the doublet [Ref. 5]. Experimentally, this is exactly what is done when the integrated intensity of an unresolved doublet is measured.

The cell lattice parameter, a , was backed out of the X-Ray diffraction patterns. For the body-centered cubic

TABLE II

R-FACTOR SAMPLE CALCULATIONS: MARTENSITE

{002-200} Martensite doublet
(Calculations based on BCC cell structure)

$2\theta = 65.1$ from diffraction pattern

$\sin\theta/\lambda = (\sin 32.55)/1.54178 = 0.349$

Element	Wt%	$f + \Delta f$	Wt. Frac	λ/λ_k
Mn	0.30	$13.82 - 0.6 = 13.22$	0.040	0.813
Si	0.25	$7.69 + 0.2 = 7.89$	0.020	0.229
Cr	4.10	$13.17 - 0.2 = 12.97$	0.532	0.745
Mo	4.25	$25.59 - 1.5 = 24.09$	1.024	2.488
V	1.10	$12.52 + 0.0 = 12.52$	0.138	0.679
Fe	90.0	$14.47 - 1.2 = 13.27$	11.943	0.884

$$f' = 13.697$$

$$FF = \{E(f')\}^2 \text{ where } E = \# \text{ atoms per unit cell} = 2$$

$$= \{2(13.697)\}^2 = 750.43$$

$$e^{-2M} = 0.92$$

$$p = 6$$

$$LP = \{(1 + \cos^2 2A \cos^2 2\theta) / \sin^2 \theta \cos \theta (1 + \cos^2 2A)\}$$

$$A = 13.305 \text{ angle of graphite monochromator crystal}$$

$$2A = 26.61$$

$$LP = 2.60$$

$$1/v^2 = 1.798 \times 10^{-3}$$

$$R = 1/v^2 \{FF \cdot p \cdot LP\} e^{-2M} = 1.798 \times 10^{-3} \{(750.43)(6)(2.60)\} 0.92$$

$$= 19.365$$

$$\text{Similarly } R\{112-211\} = 37.556$$

TABLE III
R-FACTOR SAMPLE CALCULATIONS: AUSTENITE

{200} Austenite peak

$2\theta = 50.50$ from diffraction pattern

$\sin\theta/\lambda = (\sin 25.25)/1.54178 = 0.273$

Element	Wt%	$f + \Delta f$	Wt. Frac	λ/λ_k
Mn	0.30	$15.81 - 0.7 = 15.11$	0.045	0.812
Si	0.25	$8.53 + 0.2 = 8.73$	0.022	0.229
Cr	4.10	$15.08 - 0.2 = 14.88$	0.610	0.744
Mo	4.25	$28.98 - 1.5 = 27.48$	1.168	2.486
V	1.10	$14.35 + 0.0 = 14.35$	0.158	0.679
Fe	90.0	$16.49 - 1.2 = 15.29$	13.760	0.884
		$f' = 15.760$		

$$FF = \{4(15.760)\}^2 = 3976$$

$$e^{-2M} = 0.925$$

$$p = 6$$

$$A = 13.305 \text{ angle of graphite monochromator crystal}$$

$$LP = \{(1 + \cos^2 2A \cos^2 2\theta) / \sin^2 \theta \cos \theta (1 + \cos^2 2A)\} = 4.4629$$

$$1/v^2 = 4.53 \times 10^{-4}$$

$$R = 4.53 \times 10^{-4} \{ (3976)(6)(4.4689) \} 0.95 = 45.891$$

Similarly $R\{220\} = 25.559$
 $R\{311\} = 30.350$

martensite, data for this calculation was taken from a hardened coupon that had also been tempered. The following equation, which is simply a rearrangement of Bragg's Law, was used to calculate a:

$$a = \{1.54178 * (h^2 + k^2 + l^2)^{1/2}\} / 2\sin(2\theta/\theta) \quad (\text{eqn. 2.4})$$

where:

1.54178	wavelength in angstroms of Cu radiation
h,k,l	indices of appropriate reflecting planes
2 θ	angular position of the reflection from the diffraction pattern

III. RESULTS AND DISCUSSION

Larson [Ref. 3] showed that thermomechanical processing by warm rolling refines the microstructure of M-50 steel. His work in conjunction with that of Butterfield [Ref. 6] has shown that carbides may be refined to a size of 0.2 μm and grain size to approximately 1.0 μm as compared to typically 3 μm carbide and 16 μm grain sizes in the as-received, spheroidize-annealed material. Such a microstructure is a refined version of the as-received, spheroidize-annealed material and for an application such as in a bearing, would need to be hardened.

A direct result of this refinement is a much increased ferrite grain boundary area and interfacial area between carbides and the ferrite matrix. Since austenite nucleation occurs preferentially along grain boundaries, austenitization would be expected to be accelerated [Ref. 8]. Larson [Ref. 3] and Butterfield [Ref. 6] also showed that warm rolling refines residual carbides to a minimal extent.

Bres [Ref. 7] showed that for austenitizing temperatures up to 1108°C, warm-rolled is harder than as-received M-50 in the as-quenched condition. This result would follow from more rapid dissolution of the soluble carbides in warm-rolled material.

From Figures 3.1 and 3.2, it can be seen that for all austenitizing temperatures shown, there is a greater volume fraction of retained austenite in the warm-rolled than in the as-received material. This again would suggest that carbide dissolution is occurring faster in warm-rolled material. It is well known that the austenite retained after hardening is a function of the amount of carbon and alloying elements taken into solution during austenitization and of the lowest temperature reached during quenching which was fixed at 20°C in all cases. Additionally, the data from Figures 3.1, when compared to that from Figure 3.2, would indicate that interrupting the quench to the lowest final temperature increases the volume fraction of retained austenite. This may possibly be explained as resulting from an athermal stabilization of the austenite by interrupted quenching through a Cottrell atmosphere dislocation pinning mechanism discussed by Woehrle, et. al. [Ref. 9].

Carbon and most alloying elements serve to stabilize the austenite phase by lowering the martensite start temperature, M_s , according to the relation [Ref. 10]:

$$M_s(^{\circ}C) = 539 - 423C - 30.4Mn - 17.7Ni - 12.1Cr - 7.5Mo$$

(eqn. 3.1)

where the elements represent their respective weight fractions. From this relation it is apparent that carbon

RA VS AUSTENITIZING TEMPERATURE

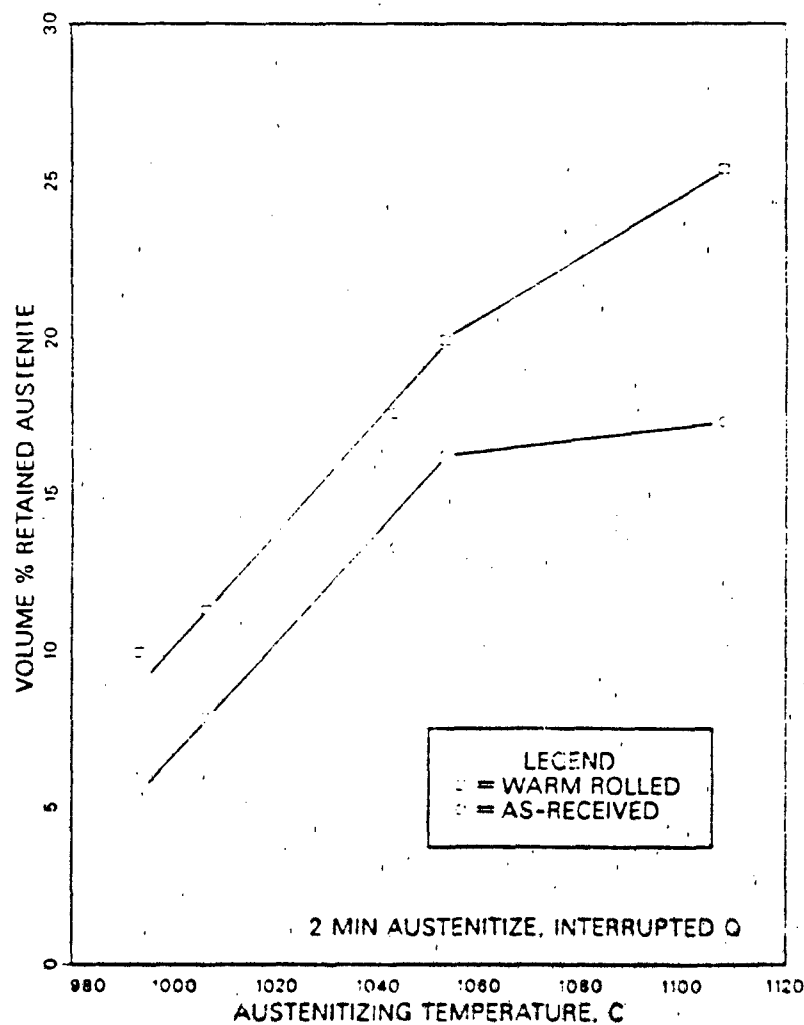


Figure 3.1. Retained Austenite (RA) as a function of austenitizing temperature for test samples quenched into molten salt at 620°C prior to air cooling to room temperature. Warm-rolled material retains more austenite in the as-quenched condition than as-received material for all austenitizing temperatures.

RA VS AUSTENITIZING TEMPERATURE

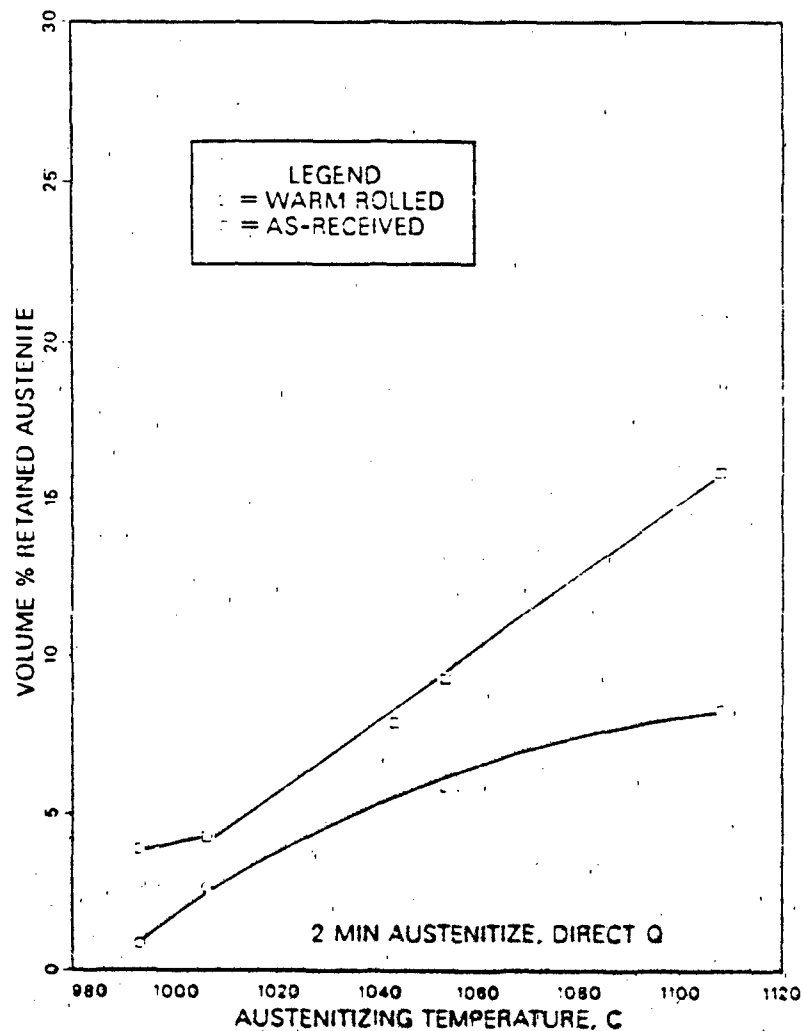


Figure 3.2. Retained Austenite (RA) as a function of austenitizing temperature for test samples directly quenched in water to room temperature. Warm-rolled material retains more austenite in the as-quenched condition than as-received material for all austenitizing temperatures.

is the single most important factor in the Ms. For this steel, carbon can theoretically lower Ms by as much as 338 centigrade degrees. On the other hand, though there are appreciable amounts of Molybdenum and Chromium in M-50, they can at most, lower Ms by only as much as 32 and 50 centigrade degrees respectively. Nevertheless, the data of Figure 3.1 and Figure 3.2 may reflect increasing solutioning of Molybdenum and Chromium as well as Carbon with increasing austenitizing temperature. For this work, the means to separate the effects of Molybdenum and Chromium from Carbon was not yet available.

From Figure 3.1, it can be inferred that equivalence in retained austenite in the as-quenched condition equates to equivalent carbon and alloy solutioning during austenitization. Accordingly, it can be seen from Figure 3.1 that the warm-rolled test coupon austenitized at 1043°C and the as-received coupon austenitized at 1108°C retained the same amount of austenite, approximately 17%.

Hardnesses of 65 Rockwell C for the as-received and 64.5 for the warm-rolled test coupons would indicate, to within the accuracy of the Wilson Hardness testing machine (± 1 Rockwell C), that both coupons are of the same hardness and that they probably contain the same amount of carbon in martensite since the as-quenched hardness is a function only of the carbon in the martensite. [Ref. 11]

Butterfield [Ref. 6] expressed concern that austenitizing warm-rolled material at around 1040°C might have led to possible overheating. However, the implication of the data presented in Figure 3.1 is that austenitizing of warm-rolled material near 1040°C is not in fact producing this result but rather an equivalent retained austenite volume fraction and therefore similar carbon in the martensite. Butterfield's micrographs indicate a finer matrix structure for this lower austenitizing temperature as compared with the microstructure of the as-received material austenitized at 1108°C .

Heavy alloying in especially Molybdenum makes M-50 a secondary hardening steel. The possible deleterious effect on the secondary hardening response of the proposed 65 centigrade degree decrease in the austenitizing temperature for the warm-rolled material was a cause for concern. In this regard, too low an austenitizing temperature may not allow sufficient solutioning of Molybdenum, whose precipitation as an M_2C type temper carbide is associated with secondary hardening [Ref. 12]. It is known, for example, that a Molybdenum-rich carbide, M_6C , does not solution until about 1088°C . On the other hand, another Molybdenum-rich carbide, metastable M_2C , dissolves at 1040°C . The tempering responses of the test coupons of interest are shown in Figure 3.3. The data shows that to within the experimental

TEMPERING RESPONSE

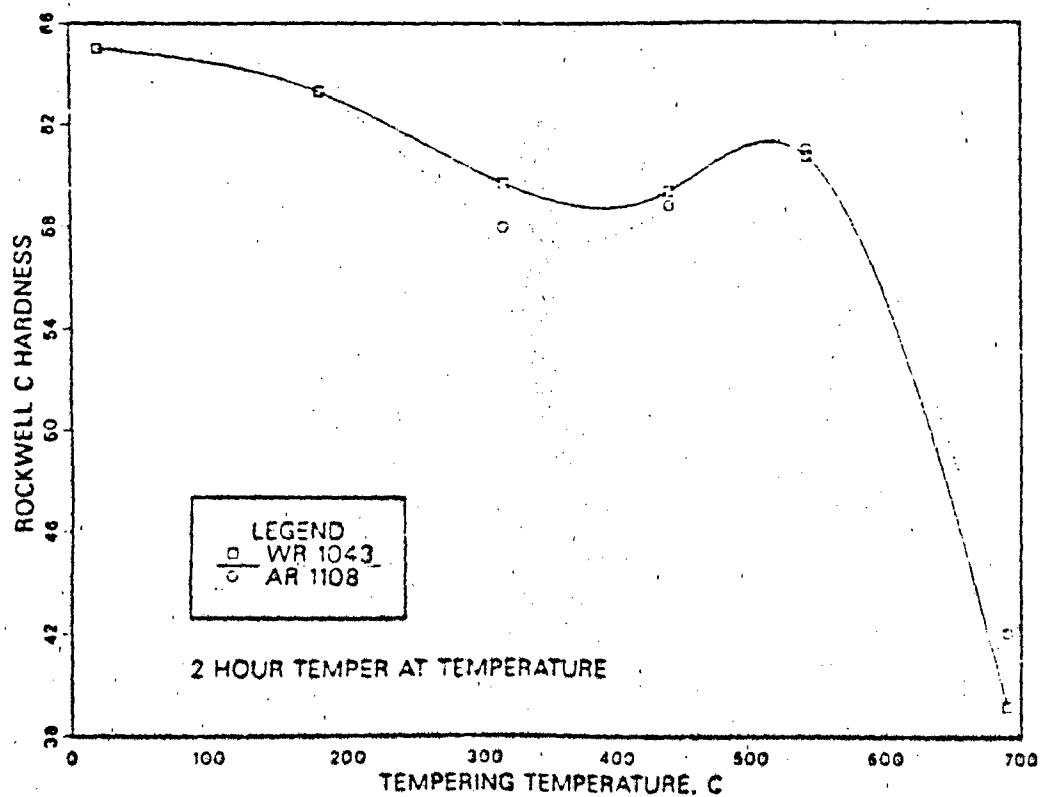


Figure 3.3. Tempering responses of the warm-rolled sample austenitized at 1043°C and the as-received sample austenitized at 1108°C. To within experimental accuracy, they are identical especially where the secondary hardening peak occurs at 61.5 Rockwell C and 540°C.

accuracy, both the as-received material austenitized at 1108°C and the warm-rolled material austenitized at 1043°C had identical secondary hardening of 61.5 Rockwell C at around 540°C. This may again be explained by the faster carbide and possibly faster alloy solutioning in warm-rolled material.

The as-received and warm-rolled samples austenitized at 1043°C did not show as big a difference in their tempering responses as was expected. However, the essential point to bring out from Figure 3.4 is that although the as-received material is only slightly softer, it is consistently so up to and through the secondary hardening peak.

When the volume fractions of retained austenite were calculated, the carbide phase was ignored and a two phase microstructure of just martensite and austenite was assumed. A probable range for the magnitude of the resultant error was estimated for the series of as-received test coupons with interrupted quenching.

To estimate these errors, the volume fractions of the phases were needed. Data on the volume fractions of the carbides of M-50 was not available but the weight fractions as a function of austenitizing temperature was available in the literature from an analysis by Bridge, et. al. [Ref. 12]. An assumption was made that the volume and weight fractions of the carbides are approximately the same. This,

TEMPERING RESPONSE

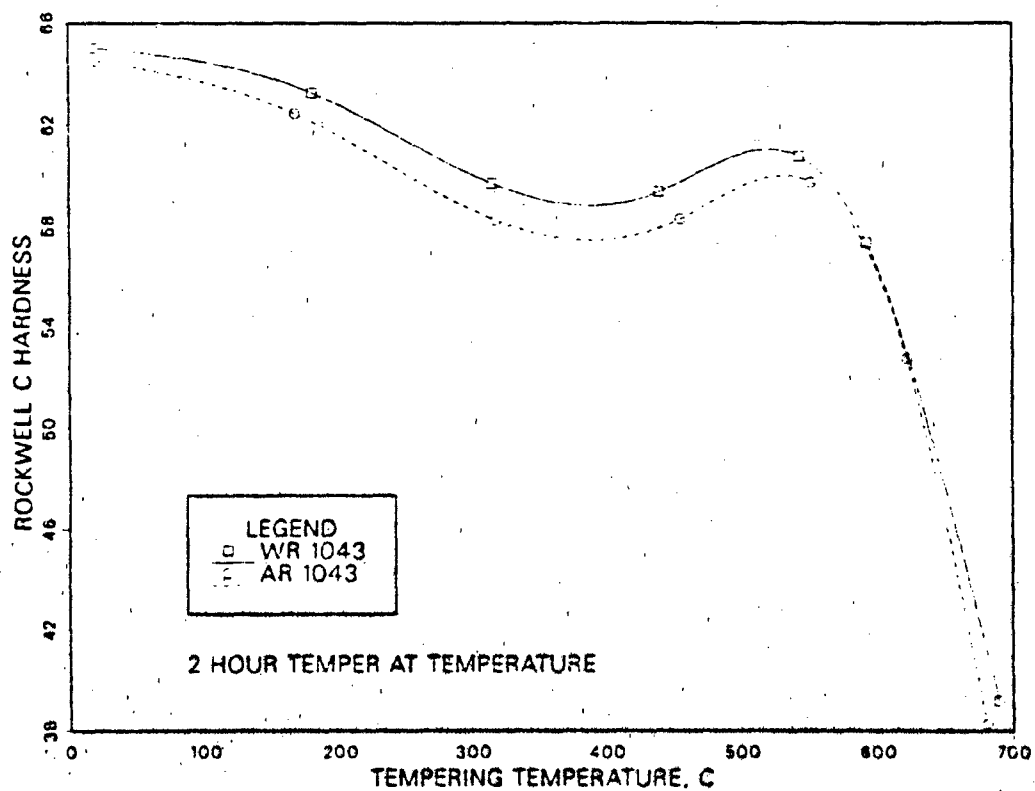


Figure 3.4. Tempering responses of the warm-rolled and as-received samples austenitized at 1043°C. Though only slightly so, the as-received sample is consistently softer.

of course, presumes that the density of the carbides is equal to that of the steel. It is believed that in reality, the carbides are not as dense as the steel and so the estimates of the error in the calculated volume fractions of retained austenite would tend to be on the high side. In point of fact, an analysis of the carbides in M2 and VASCO-MA steel as a function of austenitizing temperatures performed by Kim, et. al. [Ref. 13] showed that volume fraction parallels the plot of the data of weight fraction over the entire range of austenitizing temperatures.

The error in calculated volume fractions of retained austenite was approximated for the lowest and highest austenitizing temperatures to give an upper and lower limit on the error. The percentage error was greater at lower austenitizing temperatures because there is a larger fraction of undissolved carbides after hardening at lower as opposed to higher temperatures. Sample calculations are shown in Table IV. An upper limit of +7.6% and a lower limit of +2.9% was set for the error in the retained austenite figures.

TABLE IV

SAMPLE CALCULATION OF ERROR IN RA

From the calculated volume % RA assuming only two phases:

$$V_A = 17.33\% \quad \text{so} \quad V_M = 82.67\%$$

then

$$\frac{V_A}{V_M} = \frac{17.33}{82.67} \quad \text{or} \quad V_M = \frac{82.67}{17.33} V_A$$

Then assuming a three phase microstructure:

$$V_A + V_M + V_C = 1$$

from Bridge [Ref. 14], $V_C = 2.8\%$

so

$$V_A + \frac{82.67}{17.33} V_A + 0.028 = 1$$

Solving for V_A , $V_A = 16.84$

So the percentage error is

$$\frac{16.84 - 17.33}{16.84} \times 100 = -2.91\%$$

IV. CONCLUSIONS AND RECOMMENDATIONS

A. CONCLUSIONS

- 1) Warm rolling enhances austenitization and carbide dissolution during final hardening.
- 2) Interrupting the quench from the austenitize stabilizes the austenite phase and results in greater volume fractions of retained austenite in the as-quenched condition.
- 3) Warm-rolled M-50 can be austenitized at 1043°C to produce equivalent as-quenched and secondary hardnesses as as-received M-50 austenitized at 1108°C .

B. RECOMMENDATIONS

- 1) Use TEM to characterize the microstructural constituents, particularly the carbides.
- 2) Use X-Ray techniques to determine the amount of carbon in the matrix.

LIST OF REFERENCES

1. Sherby, O. D., "Superplasticity, Ultra High Carbon (UHC) Steels and UHC Steel Composites," Talk given at Lawrence Livermore Laboratory, Livermore, California, February 24, 1977, transcribed from tape and edited, March 1977.
2. McNelley, T. R., Edwards, M. R., Doig, A., Boone, D. H., Schultz, C. W., "The Effects of Prior Heat Treatments on the Structure and Properties of Warm-Rolled AISI 52100 Steel," Metallurgical Transactions, v. 14A, pp. 1427-1433, July 1983.
3. Larson, K. R., Jr., Thermomechanical Processing of M-50 Steel, Naval Postgraduate School, Monterey, California, 1983.
4. Society of Automotive Engineers Information Manual SP-453, Retained Austenite and Its Measurement by X-Ray Diffraction, by C. H. Jaczak, J. A. Larson, and S. W. Chin, January 1980.
5. Cullity, B. D., Elements of X-Ray Diffraction, Addison-Wesley, 1956.
6. Butterfield, F. A., Rolling Contact Fatigue Testing of Thermomechanically Processed M-50 Steel, M.S. Thesis, Naval Postgraduate School, Monterey, California, 1984.
7. Bres, E. V., The Heat Treatment Response of Thermomechanically Processed M-50 Steel, M.S. Thesis, Naval Postgraduate School, Monterey, California, 1983.
8. Shewmon, P. G., Transformations in Metal, McGraw-Hill, 1969.
9. Woehrlé, H. R., Clough, W. R., and Ansell, G. S., "Athermal Stabilization of Austenite," Transactions of the ASM, v. 59, pp. 785-803, 1966.
10. Andrews, K. W., "Empirical Formulae for the Calculation of Some Transformation Temperatures," Journal of the Iron and Steel Institute, pp. 721-727, July 1965.
11. Brick, R. M., Gordon, R. B., and Philips, A., Structure and Properties of Alloys, McGraw-Hill, 1965.

12. Bridge, J. E., Jr., Maniar, G. N., and Philip, T. V., "Carbides in M-50 High Speed Steel," Metallurgical Transactions, v. 2, pp. 2209-2214, August 1971.
13. Kim, C., Biss, V., and Hosford, W. F., "A New Procedure for Determining Volume Fraction of Primary Carbides in High-Speed and Related Tool Steels," Metallurgical Transactions, v. 13A, pp. 185-191, February 1982.

INITIAL DISTRIBUTION LIST

	<u>No. Copies</u>
1. Defense Technical Information Center Cameron Station Alexandria, Virginia 22314	2
2. Library, Code 0142 Naval Postgraduate School Monterey, California 93943	2
3. Department Chairman, Code 69 Department of Mechanical Engineering Naval Postgraduate School Monterey, California 93943	1
4. Dr. T. R. McNelley, Code 69Mc Department of Mechanical Engineering Naval Postgraduate School Monterey, California 93943	2
5. Commander (Attn: Dan Popgoshev) Naval Air Propulsion Center P.O. Box 7176 Trenton, New Jersey 08628	2
6. Commander (Attn: Ron Dayton) Air Force Wright Aeronautical Laboratories Wright-Patterson Air Force Base Dayton, Ohio 45433	2
7. LT Nestor H. Camerino, Jr. c/o C. H. Camerino 430 De Mar Drive Sacramento, California 95831	2

END

DATE
FILMED

8 - 85

DTIC